Nano Energy (▮▮▮▮) ▮, ▮▮▮–▮▮▮

Available online at www.sciencedirect.com

ScienceDirect

journal homepage: www.elsevier.com/locate/nanoenergy

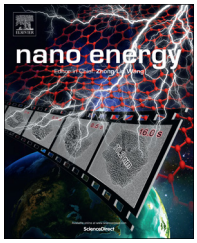

First principle simulations of piezotronic transistors

Q1 Wei Liu[a], Aihua Zhang[a], Yan Zhang[a,b,*], Zhong Lin Wang[a,c,*]

[a]Beijing Institute of Nanoenergy and Nanosystems, Chinese Academy of Sciences, Beijing 100083, China
[b]Institute of Theoretical Physics, and Key Laboratory for Magnetism and Magnetic Materials of MOE, Lanzhou University, Lanzhou 730000, China
[c]School of Material Science and Engineering, Georgia Institute of Technology, GA 30332, USA

Received 4 September 2014; received in revised form 30 September 2014; accepted 2 October 2014

KEYWORDS
Piezotronic transistor;
First principle simulations;
Width of piezoelectric charge distribution;
Modulation of Schottky barriers

Abstract
Piezoelectric semiconductors, such as wurtzite structured ZnO, GaN, and InN, have novel properties owing to piezoelectric polarization tuned/controlled electronic transport characteristics. Under an externally applied strain, piezoelectric charges are created at an interface or junction, which are likely to tune and modulate the local band structure. Taking an Ag-ZnO-Ag two-terminal piezotronic transistor as an example, strain-dependent piezoelectric charge distributions and modulation of Schottky barrier heights (SBHs) at metal/semiconductor interfaces have been investigated by the first principle simulations. The width of piezocharge distribution is calculated by the density function theory and the Poisson equation. The modulations of SBHs at two interfaces show opposite trend under the applied strain. This study not only provides an understanding about the piezotronic effect from quantum theory point of view, but also a new method to calculate the key parameter for optimizing the design of piezotronic devices.

Introduction

Piezoelectric semiconductor materials, such as wurtzite ZnO, GaN, InN, and CdS, have drawn intensive research interests for fabricating functional electronics [1-3]. Under an externally applied mechanical strain, piezoelectric charges (piezocharges) are created at a metal-semiconductor interface or a *pn* junction, which are likely to tune the local Schottky contact or charge-depletion zone and can be used as a new means for "gating" carrier transport. This is a new emerging field of piezotronics [4]. Piezotronic effect has been studied and utilized for two-terminal strain gated transistors [5,6], logic devices [7], memory units [8], enhancing solar cell and LED efficiency [9,10], enhanced gas/chemical/bio-sensing [11-13], and straining mapping [14]. Recently, array and chip based piezotronic devices have been developed as flexible human-machine interfacing [15]

Q2 *Corresponding author's at: Beijing Institute of Nanoenergy and Nanosystems, Chinese Academy of Sciences, Beijing 100083, China
E-mail addresses: zhangyan@lzu.edu.cn (Y. Zhang), zlwang@gatech.edu (Z.-A. Lin Wang).

http://dx.doi.org/10.1016/j.nanoen.2014.10.014
2211-2855/

and photonic-strain mapping [16], setting a milestone from fabricating single devices to an array of devices and even to an integrated system [17].

Theoretical studies have been carried to understand the fundamentals of piezotronics using semi-classical models, including piezopotential distribution in strained ZnO nanowires [18,19], the influence of piezopotential spatial distribution on local contact dictated transport properties of ZnO nanowires [20], and the establishment of theoretical framework of piezotronics for qualitative understanding carrier transport behavior [21]. Recently ab initio simulations studies are employed to investigate the piezoresistance effect with the change in bandgap under strain for the nanoscopic transistor [22,23]. Piezoresistance effect is a volume based effect without polarity that is a common feature for almost any semiconductors. However, piezotronic effect is a result of piezoelectric charges at the local interface that has strong polarity dependence, thus, exhibiting an asymmetric or non-symmetric effect on the local contacts at the ends of a wurtzite or zinc-blende structured material. From our previous theoretical work [21], the width of piezoelectric charge distribution at the local interface is an important factor for piezotronics, but such information cannot be provided by the classical piezotronic theory although we believe that the charge distribution is within a few atomic layers. The ab initio methods are computational methods from first principles of quantum mechanics, and used for calculating atomic and molecular structure based entirely on quantum mechanics and basic physical constants. Density functional theory (DFT) method is one of the most important ab initio methods for calculating molecules electronic structure. DFT simulation can provide quantitative information about the width of piezoelectric charges at the interface and their distributions depending on the piezoelectric semiconductor material and crystal structure.

In this article, we present the first ab initio calculation on the piezotronic effect in a metal-semiconductor-metal based two-terminal piezotronic transistor. The distribution of piezoelectric charge density at the metal-semiconductor interface is investigated and its influence on the local Schottky barrier height is studied. By using the density functional theory, the electrostatic potential within the transistor can be obtained. Then the Poisson equation is employed to calculate the charge density from the electrostatic potential. Based on the charge density, the piezoelectric charge distribution and the total piezoelectric charge versus strain are calculated. Furthermore, the modulation of Schottky barrier height by the piezotronic effect is calculated in the interface region under the strain. Our study provides the first quantum mechanical understanding about piezotronic effect and establishes its physics bases starting from first principle. This study is important for quantitative understanding the effect and optimized design of piezotronic devices.

Model and method

To illustrate the first-principles calculations based on the DFT simulation for the piezotronics, a typical metal-semiconductor-metal (MSM) piezotronic transistor is taken as an example. Figure. 1 shows an Ag-ZnO-Ag transistor, including the center ZnO sandwiched between the left-hand and right-hand side Ag electrodes. In our model, ZnO has a hexagonal wurtzite structure, with its *c*-axis chosen pointing from the left to the right Ag electrode, as shown in Figure. 1. The Ag(1 1 1) plane is assumed to directly interfacing with the $\pm$(0001) polar planes of ZnO. The atomic structure of ZnO and Ag are also given in Figure. 1: the white ball denotes to Zn atom, red ball for O atom, and blue ball for Ag atom. According to the classical piezotronics theory, when a tensile strain along the *c*-direction is applied on the transistor, negative piezoelectric charges are created at the $-c$ side of the metal-semiconductor (M-S) interface (ZnO($000\bar{1}$)-Ag junction), while positive charges are created at the $+c$ side (ZnO(0001)-Ag junction). Alternatively, the signs of charges reverse when a compressive strain is applied. Positive piezoelectric charges induce positive piezoelectric potential and lower the barrier height at the local contact, while negative charges induce negative potential and raise the barrier height.

A lateral view of the Ag-ZnO-Ag piezotronic transistor is shown in Figure. 2(a) without applying strain. In the present study, the transistor consists of four double (eight single) Zn-O layers as center region and Ag(1 1 1) layers on the left-hand ($000\bar{1}$) and right-hand (0001) side of ZnO, respectively, as two electrodes. ZnO{0001} direction and Ag(1 1 1) plane parallel to *c* axis and *a*-*b* plane of the transistor supercell, respectively. Four planes represented by black dashed lines in parallel to Ag(1 1 1) plane, A, B, C, and D, divide the transistor into three regions: AB is the left-hand electrode contacting to ZnO($000\bar{1}$)-O polar surface, CD is the right-hand one contacting ZnO(0001)-Zn polar surface, and BC is the center ZnO region [24]. The periodical boundary condition is applied to all *a*, *b*, and *c* directions of the supercell; the box in Figure. 2(a) shows the supercell of the transistor used for the calculation. For simplicity, we neglect the effect of impurity/defect in our transistor model. Considering that metal films are more flexible, on the basis of a commonly adopted method for constructing the interface model [25]: the in-plane lattice constants of the transistor supercell is chosen as the same as those of the bulk ZnO. For simplicity, such treatment is applied by elongating the in-plane lattice constants of Ag(1 1 1) layers in order to eliminate the lattice mismatch between the two materials in our model. By using the treatment in previous theoretical study [22,23,25], the theoretical model is stable and has a simple structure. Therefore, the treatment simplifies the complexity of calculations. The structure of the Ag/ZnO interface is assumed as follows [25-28]: for ZnO($000\bar{1}$)-Ag interface (Ag-O polar surface), Ag atoms tend to lie on the

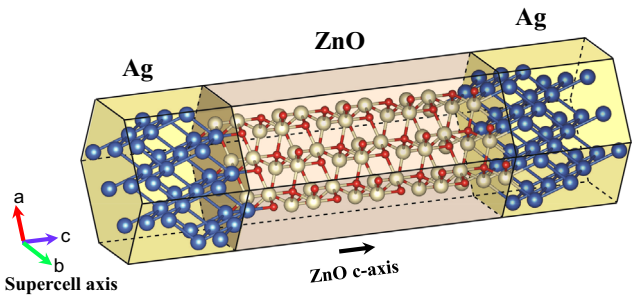

Fig. 1 Schematic illustration of a Ag-AnO-Ag piezotronic transistor and its atomic structure model, with the *c*-axis of ZnO is indicated.

Please cite this article as: W. Liu, et al., First principle simulations of piezotronic transistors, Nano Energy (2014), http://dx.doi.org/10.1016/j.nanoen.2014.10.014

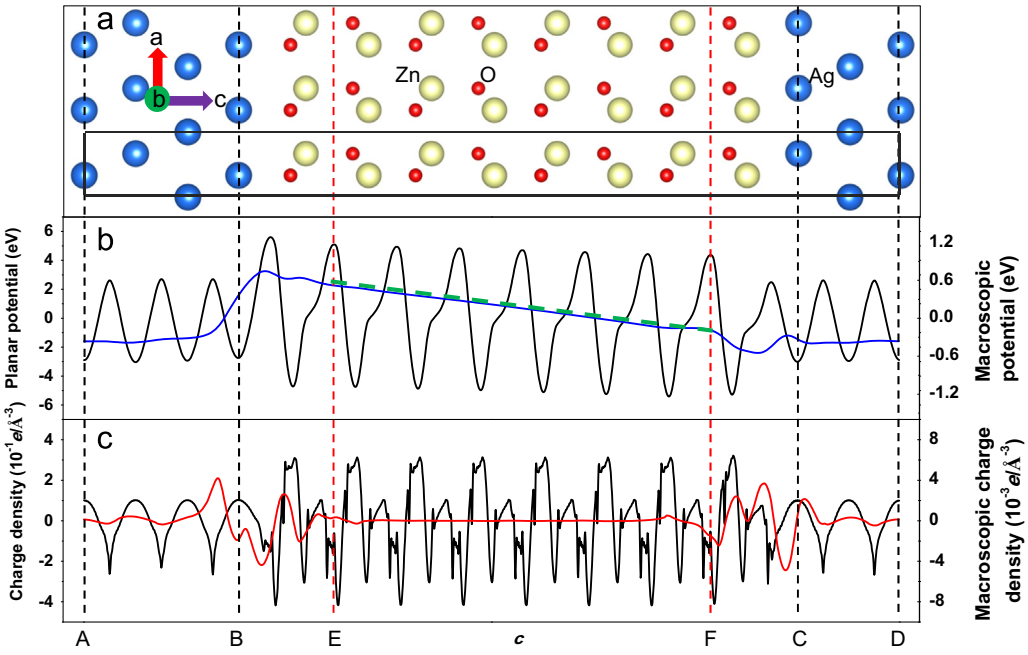

Fig. 2 (a) Projected schematic atomic structure of the hcp-Ag-ZnO-Ag piezotronic transistor. (b) The planar average electrostatic potential of the transistor (black line). The double macroscopic average of planar electrostatic potential and linear fit of potential in inner ZnO region are denoted by blue line and green dashed line, respectively. (c) The planar averaged total charge density of the transistor (black line), which is obtained as the 2nd derivative of the planar electrostatic potential (Poisson equation). The macroscopic averaged total charge density is denoted by a red line.

top of O atoms [25]; for ZnO(0001)-Ag interface (Ag-Zn polar surface), two typical structures in ZnO(0001) surface are stable for accommodating Ag atoms: hcp and fcc hollows [25-28]. Therefore, the transistor has two typical structures: *hcp*- and *fcc*-Ag-ZnO-Ag according to the type of Zn-Ag contact. Figure. 2(a) shows the hcp-Ag-ZnO-Ag transistor supercell. Based on the DFT method, the constructed piezotronic transistor supercell can be calculated to obtain the equilibrium structure with minimum energy. After optimization, the resulting lattice constants and relaxed atomic coordinates of piezotronic transistor supercell are obtained. The construction and optimization of initial structure consists of the following steps [23]: (1) optimize the bulk ZnO as well as Ag with fixing its in-plane constant same to that of bulk ZnO; (2) construct Ag-ZnO-Ag piezotronics transistor, by using the optimized structure of ZnO and Ag, and optimize the interfacial layer distances between ZnO and Ag; (3) all atoms in transistor system and lattice constants are fully relaxed to obtain the optimized structure without applied external strain.

The structure optimization of the Ag-ZnO-Ag piezotronic transistor is based on DFT. The exchange correlation potentials are treated by the Perdew-Burke-Ernzerhof (PBE) parameterization within the general gradient approximation (GGA) [29], which is implemented in the Vienna ab initio simulation package (VASP) [30,31] with the frozen-core projector-augmented-wave (PAW) pseudopotentials [32,33]. In a periodic system, the electron density is calculated by performing the integrations of electronic wave functions over the first Brillion zone. However, in the practical calculation, the integrations are calculated by numerical integration of electronic wave functions at a finite k-point mesh in the Brillion zone. A k-point sampling by the $9 \times 9 \times 9$ mesh for the bulk ZnO and Ag(1 1 1) unit cells and a $9 \times 9 \times 3$ mesh for the transistor supercell are adopted in the present simulation [23,25]. In VASP software package, a plane-wave basis set is employed to expand the electronic wave function at each k-point. In practice, an infinite number of plane-waves is applied for the expansion in DFT calculation. However, the expansion coefficients of plane-waves with small kinetic energies are more important than plane-waves with large kinetic energies. Therefore, the plane-waves basis set can be truncated to contain plane waves with the kinetic energies less than a particular cutoff energy [34]. In the current study, the cutoff kinetic energy is chosen as 500 eV.

An external strain (from −5% to 5%) is applied along the *c* axis [22,35]. In our calculation, the strain can be typically applied in two ways: (a) only the center region, (BC in Figure. 2(a)), is under strain, and (b) the whole transistor is under strain. The structure relaxation is performed on the atoms under the strain. Structures obtained by methods

Please cite this article as: W. Liu, et al., First principle simulations of piezotronic transistors, Nano Energy (2014), http://dx.doi.org/10.1016/j.nanoen.2014.10.014

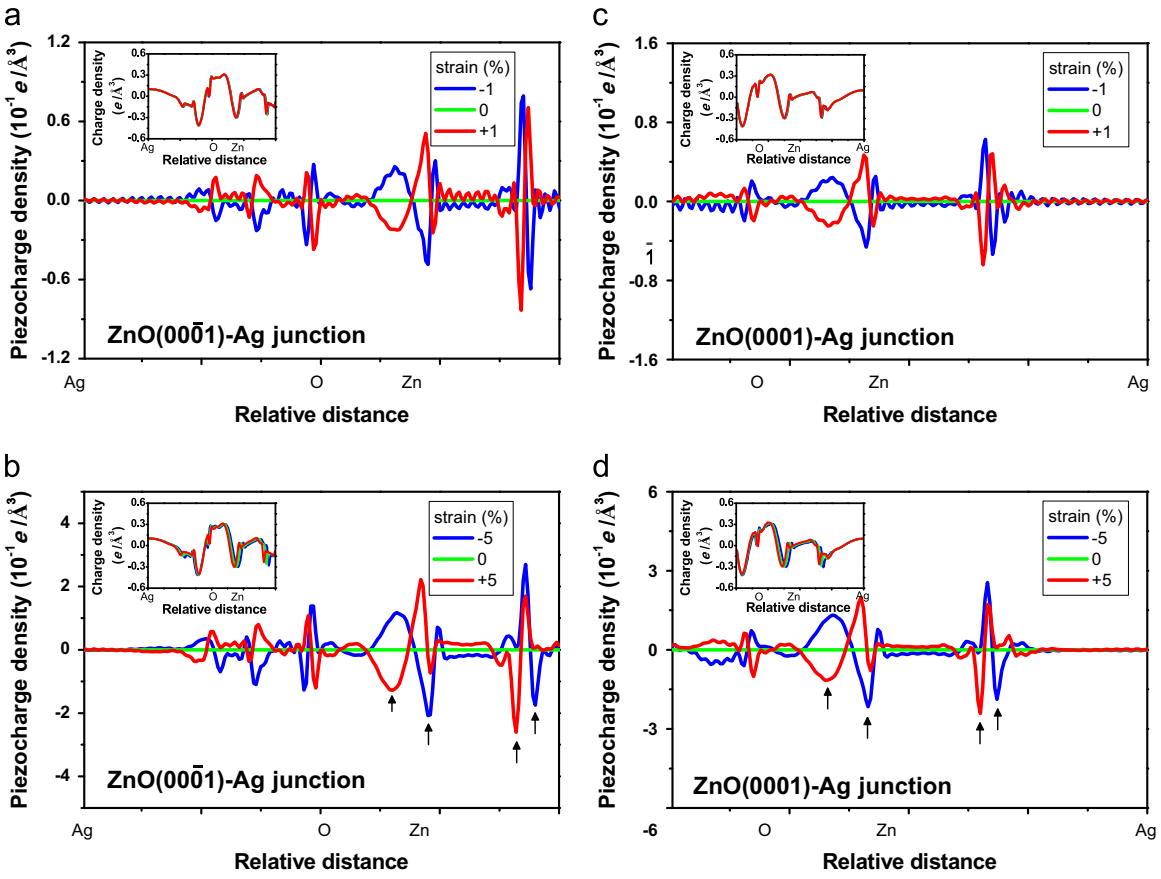

Fig. 3 Piezoelectric charge distributions at interface regions of hcp-Ag-ZnO-Ag transistor: (a) ZnO(000$\bar{1}$)-Ag interface under strains $\pm$1%, (b) ZnO(000$\bar{1}$)-Ag interface under strains $\pm$5%, (c) ZnO(0001)-Ag interface under strains $\pm$1%, and (d) ZnO(0001)-Ag interface under strains $\pm$5%. The insets are *absolute* charge distributions. e is absolute electron charge, $e=1.6\times10^{-19}$ C.

(a) and (b) give similar results (refer to Figures. s1-s6), which are given as supporting information. Therefore, the transistor structure is optimized using method (a) in the discussion below. Furthermore, we also construct transistors with longer ZnO and Ag region. Upto 15 double layers ZnO are included in these transistors and the length of each electrode is upto 6 Ag layers. The piezoelectric charge distribution and Schottky barrier heights (refer to Sects. 3 and 4 below) obtained from these transistors do not show obvious difference from the shorter ones, indicating the stability of our calculation.

The piezoelectric charge distribution is calculated by using the *a-b* planar-averaged total charge density, so that it is a one-dimensional function depending on the z along the *c* axis of the supercell, which is obtained from the planar-averaged electrostatic potential by using Poisson's equation. The electrostatic potential of electron within the transistor region is calculated by VASP. By averaging the electrostatic potential in *a-b* plane of the supercell, the obtained planar averaged electrostatic potential [25] (referred to below as *planar potential*) of hcp-Ag-ZnO-Ag transistor is shown in Figure. 2(b) as a black line. The blue line presents the average potential obtained by double-macroscopic-average method [36,37] (referred to below as *macroscopic potential*), for filtering out the charge density fluctuations that follow the underlying atomic structures in both deep Ag and ZnO region [23]. Since it lacks center symmetry in ZnO wurtzite structure, a built-in electric field exists in deep ZnO region, resulting in a non-flat macroscopic potential. By the linear extrapolation, the macroscopic potential can be used in calculating the modulation of Schottky barrier heights due to the piezotronic effect.

The planar charge density ρ in the transistor region, which is shown as a black line in Figure. 2(c), can be obtained by applying the Poisson's equation:

$$\frac{\partial^2 U}{\partial z^2} = -\frac{\rho}{\varepsilon} \tag{1}$$

Here U is the planar potential shown in Figure. 2(b), z parallels to *c* axis, and ε the permittivity of free space. It is worth noting that the (planar averaged) electrostatic potential of electron includes two parts: one is the ionic potential which is in the form similar to classical electrodynamics; the other is the Hartree potential which rises from the electron charge density and is calculated from the Poisson's equation in VASP [33]. Thus the Poisson's equation is eligible for calculating the total charge density in the present study. In calculating of the planar potential and the charge density, a 2000-point mesh along *c* axis is adopted for the whole transistor. The charge in each mesh is obtained as the integration of the charge density in mesh volume. Since the supercell is electro-neutral, the total amount of charge in supercell must be zero in our simulation.

Please cite this article as: W. Liu, et al., First principle simulations of piezotronic transistors, Nano Energy (2014), http://dx.doi.org/10.1016/j.nanoen.2014.10.014

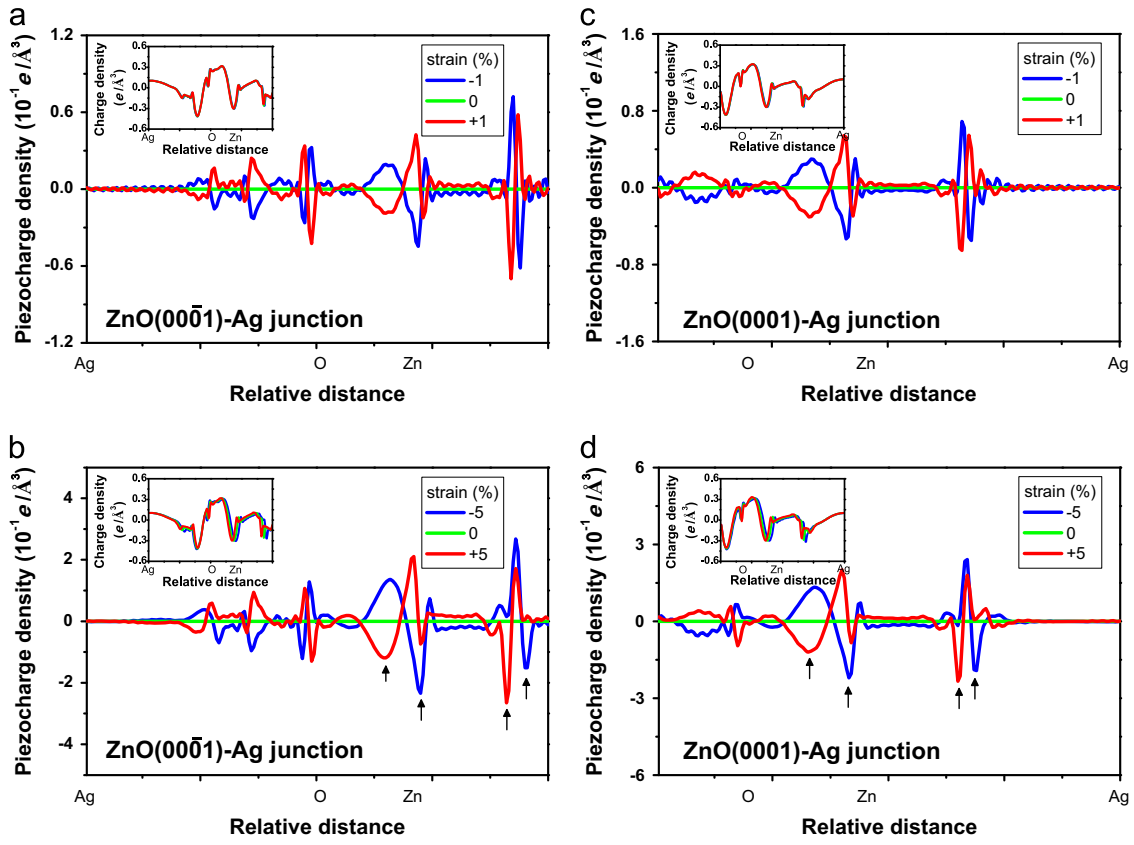

Fig. 4 Piezoelectric charge distributions at interface regions of the fcc-Ag-ZnO-Ag transistor: (a) ZnO(000$\bar{1}$)-Ag interface under strains $\pm$1%, (b) ZnO(000$\bar{1}$)-Ag interface under strains $\pm$5%, (c) ZnO(0001)-Ag interface under strains $\pm$1%, and (d) ZnO(0001)-Ag interface under strains $\pm$5%. The insets are *absolute* charge distributions. e is absolute electron charge, $e=1.6\times10^{-19}$ C.

The center ZnO region includes eight Zn-O single layers. The charge density of the 1st and 8th layers are different from those of the inner layers, as shown in Figures. 2(b) and 2(c), due to the influence of the Ag electrodes on Ag-O polar surface for the 1st layer and Ag-Zn polar surface for the 8th layer. According to our calculation, the macroscopic potential distribution in ZnO region can be divided into three parts, a linear and two nonlinear regions, as shown in Figure. 2(b). From Poisson's equation, there is no charge in the linear region. Nonlinear regions indicate macroscopic charge distribution (refer to the red line in Figure. 2(c), which denotes the macroscopic charge density). Then the center ZnO region is further divided into three parts: the left interface BE, the right interface FC, and the inner ZnO region (EF).

The methodology, approximations and approach presented above are adopted for both hcp- and fcc-Ag-ZnO-Ag transistor, including the structure optimization, the exertion of strain, the calculation of planar as well as macroscopic potential, and the chosen of inner ZnO and interface region.

Piezoelectric charge distribution at the interface region

For both hcp- and fcc-Ag-ZnO-Ag transistors, the calculated charge distributions at the interface regions show obvious atomic scale fluctuation (refer to the insets of Figures. 3 and 4). From classical piezoelectric theory, piezoelectric charges created by the applied strain equal to the charge difference between the device with and without the applied strain. Thus, we calculate the charge difference for studying piezoelectric charge distribution, as shown in Figures. 3 and 4 for hcp- and fcc-transistors, respectively. It is found that the distributions of the piezocharges are similar to each other for two typical structures: hcp- and fcc-transistors. However, the piezocharge distribution in the ZnO(000$\bar{1}$)-Ag and ZnO(0001)-Ag interface regions are different from each other in each transistor, which is due to the asymmetric contact geometry of two interface regions. Using the charge difference technique, the piezoelectric charge distributions show obvious dependence according to the sign of applied strain (tensile/compressive). When the strain is small, $\pm$1% for example, the large peaks value under +1% tensile strain are approximately equal to those under $-$1% compressive strain, but with opposite sign as shown in Figures. 3(a), 3(c), 4(a) and 4(c) by black arrowheads. However, when the strain becomes larger, $\pm$5% for instance, the relative positions of the large peaks under +5% strain shift from those under $-$5% strain, as indicated by black arrowheads in Figures. 3(b), 3(d), 4(b) and 4(d). According to the classical piezoelectric theory, piezoelectric charges are assumed to distribute at the very interface, which is expected to be within one or two atomic layers. In our DFT simulation, the calculated total charges at the interface region agree with this assumption and show significant dependence on the applied strain. The widths of the piezocharges are about 4.1 Å at ZnO(000$\bar{1}$)-Ag junction side and 3.7 Å at ZnO(0001)-Ag junction side, which

Please cite this article as: W. Liu, et al., First principle simulations of piezotronic transistors, Nano Energy (2014), http://dx.doi.org/10.1016/j.nanoen.2014.10.014

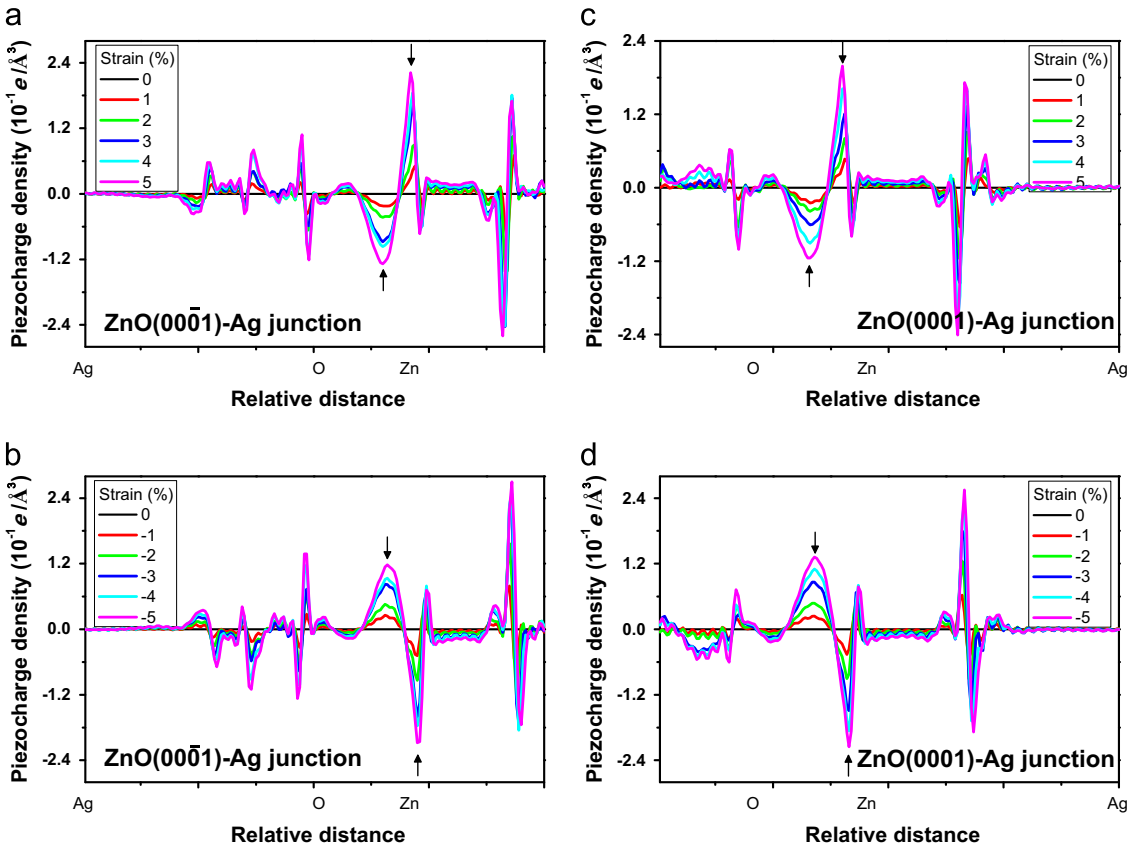

Fig. 5 Dependence of piezoelectric charge distribution on strain in hcp-Ag-ZnO-Ag transistor: (a) ZnO(000$\bar{1}$)-Ag interface under strains from 1% to 5%, (b) ZnO(000$\bar{1}$)-Ag interface under strains from −1% to −5%, (c) ZnO(0001)-Ag interface under strains from 1% to 5%, and (d) ZnO(0001)-Ag interface under strains from −1% to −5%.

are assumed to be 2.5 Å in the previous theoretical study [21]. Such difference in the widths of piezocharges is due to the different layer distances between ZnO(000$\bar{1}$)-Ag and ZnO (0001)-Ag, indicating that the width of piezocharges depends on the type of electrode metal. Figures. 5 and 6 reveal the evolution of the interface piezocharges with increasing/decreasing external applied strain in hcp- and fcc-transistor, respectively. Large peaks can be found near the middle of Ag and Zn atoms as well as in the vicinity of O atoms. The distribution of the piezocharges is abrupt and strain-dependent. For each case, the piezocharge distribution has a similar trend under tensile/compressive strain in either ZnO (000$\bar{1}$)-Ag or ZnO(0001)-Ag interface. Increasing the tensile/compressive strain does not obviously change the distribution structure of the piezoelectric charges, but to increase the peak value, as indicated by the black arrow in Figures. 5 and 6.

The total amount of piezoelectric charges density in ZnO (000$\bar{1}$)-Ag/ and ZnO(0001)-Ag interface regions are calculated under various strains, as shown in Figure. 7 for hcp- and fcc-transistors. Both transistors give similar trends. The total piezocharge shows obvious linear dependence on applied strain at both interfaces. In the case of ZnO(000$\bar{1}$)-Ag interface region, positive charges increases under compressive strain, while negative charges increase under tensile strain, as shown in Figures. 7(a) and 7(c). On the other hand, the case of ZnO (0001)-Ag interface region is vice versa: negative charge increases under compressive strain and positive charge increases under tensile strain, as shown in Figures. 7(b) and 7(d). Besides the interface regions, we have also calculated the total charges in deep Ag (AB and CD) and ZnO (EF) regions. The strain-dependent variations of the total charges in these regions are negligible compared with those in interface regions, indicating that only the total charges in the interface regions effectively depend on the applied strain. The above results are consistent to that of the clas;sical piezotronics theory [21] and the experimental measurements.

Schottky barrier heights

Piezotronic effect is about the piezoelectric charge tune/control carries transport process under an applied strain. In the case of M-S contact, the piezoelectric charges will change Schottky Barrier Heights (SBHs), which strongly dictate the electronic transport characteristics of the piezotronic device. The n-type SBH (Φ_B) can be obtained in Ag/ZnO interface using the bulk-plus-lineup method [25,38-40]:

$$\Phi_B = E_g - [E_F - E_V] = E_g - [E_F - (\overline{V} + \Delta)], \quad (2)$$

where E_g is the band gap of bulk ZnO, E_F the Fermi level of the Ag-ZnO-Ag transistor, $\overline{V}$ the macroscopic averaged potential in the interface region, and Δ the energy difference between the valence band edge and the averaged potential in bulk ZnO. Under a certain applied strain, E_g, E_F, and Δ for SBHs of both ZnO(000$\bar{1}$)-Ag and ZnO(0001)-Ag interfaces have the same

Please cite this article as: W. Liu, et al., First principle simulations of piezotronic transistors, Nano Energy (2014), http://dx.doi.org/10.1016/j.nanoen.2014.10.014

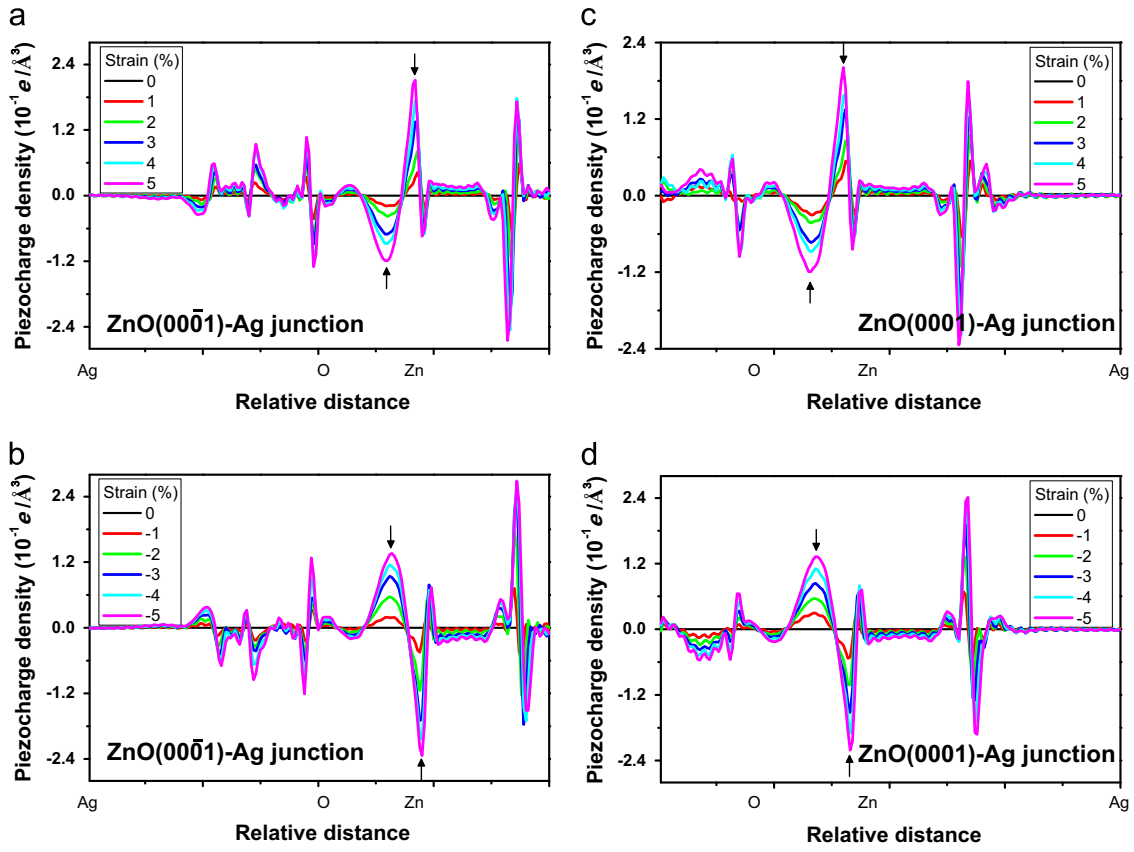

Fig. 6 Dependence of piezoelectric charge distribution on strain in fcc-Ag-ZnO-Ag transistor. (a) ZnO(000$\bar{1}$)-Ag interface under strains from 1% to 5%, (b) ZnO(000$\bar{1}$)-Ag interface under strains from −1% to −5%, (c) ZnO(0001)-Ag interface under strains from 1% to 5%, and (d) ZnO(0001)-Ag interface under strains from −1% to −5%.

value. So they reflect the piezoresistance effect which is symmetric for two contacts. On the other hand, $\overline{V}$ is affected by the variation of electric field under the applied strain, hence reflecting the piezotronics effect. In the present study, we focus on the relative change of SBH due to the piezotronic effect, namely$\Delta SBH_{piezo} = \Delta\overline{V}$. In our simulation, the obtained electrostatic potential is normalized, so that the integration of the potential in whole supercell volume is 0. To compare $\overline{V}$ under different strains, a reference macroscopic potential is adopted, which is taken from the middle of inner ZnO region [23,25]. By linear extrapolation of macroscopic potential in the inner ZnO region, $\overline{V}$ at the two interface regions (at the middle of Ag-Zn and Ag-O in the left and right interface region, respectively) are obtained. Then $\Delta\overline{V}$ is evaluated as the difference between $\overline{V}$ with and without strain. The strain-dependent modulations of SBHs of hcp- and fcc-Ag-ZnO-Ag transistors due to the piezotronics effect are shown in Figures. 8(a) and 8(b), respectively. The modulations of SBHs of two transistors show similar behaviors versus applied strain. SBHs of the ZnO(000$\bar{1}$)-Ag interface of both transistors decrease under compressive strain, which is due to the increasing of the positive piezocharges; while SBHs of the ZnO(0001)-Ag interface increase under compressive strain, which is due to the increasing of the negative piezocharges. Alternatively, SBHs increase for the ZnO(000$\bar{1}$)-Ag interface and decrease for the ZnO(0001)-Ag interface under tensile strain. Furthermore, the behaviors of $\Delta\overline{V}$ at two interfaces indicate that the modulation of SBH is asymmetric, which have been observed by many experiments [5-8,17]. In case of 1% tensile/compressive strain, the modulations of SBHs of both type transistors are around 5 meV, which agree with the results of previous experiments [41]. Although the above results is obtained in the cases that the strain exerted only on the ZnO regions, the same conclusion holds for the case where the strain applied on the whole transistor. Figures. S1, S2, S3 and S4 show the distributions of strain-dependent charges and piezocharges at the interface regions, which are similar to those of the corresponding Figures. 3, 4, 5 and 6 that strain exerted only on the center region. In addition, the strain-dependence of the total piezoelectric charges in the interface regions and the modulation of Schottky barriers are shown in Figures. s5 and s6 respectively, also in agreement with the corresponding Figures. 7 and 8.

Summary

In summary, by employing the density functional simulation, the width of distribution of piezoelectric charges and modulation of Schottky barrier heights in two interface regions of piezotronic Ag-ZnO-Ag transistor have been calculated. The piezoelectric charges in the vicinity of O atom and between Zn-Ag atoms are calculated as a function of the applied strain. The modulation of Schottky barriers is asymmetric at the two contacts, in agreement to the reported experimental results. The strain-dependent carriers transport properties of piezotronic transistor

Please cite this article as: W. Liu, et al., First principle simulations of piezotronic transistors, Nano Energy (2014), http://dx.doi.org/10.1016/j.nanoen.2014.10.014

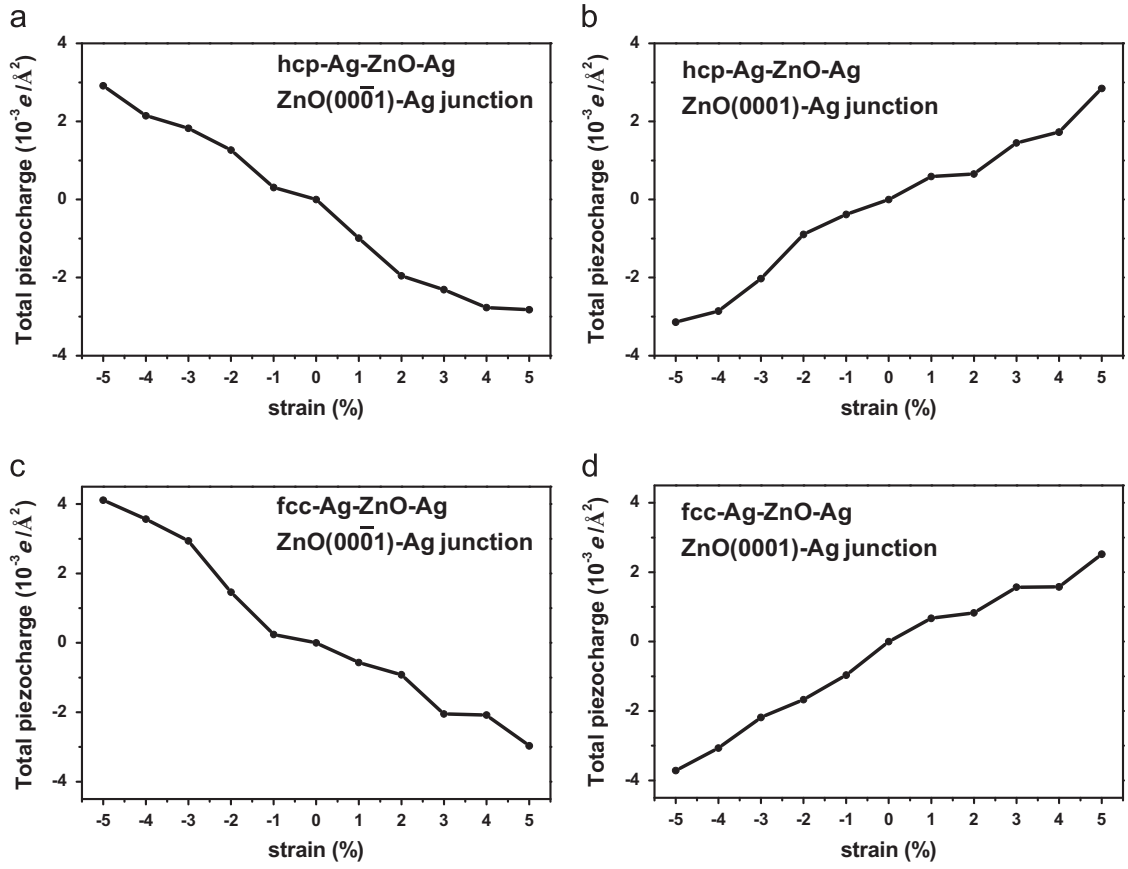

Fig. 7 Total piezoelectric charge per surface area in (a) ZnO(000$\bar{1}$)-Ag interface and (b) ZnO(0001)-Ag interface versus applied strain in hcp-Ag-ZnO-Ag transistor. (c) and (d) are corresponding ones in fcc-Ag-ZnO-Ag transistor.

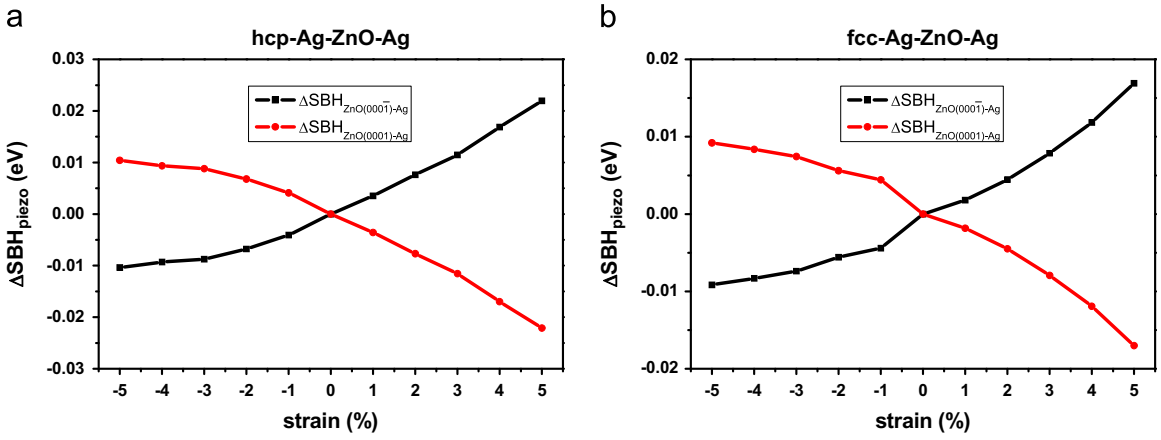

Fig. 8 Modulation of Schottky barrier heights in ZnO(000$\bar{1}$)-Ag and ZnO(0001)-Ag interfaces due to piezotronic effect in (a) hcp- and (b) fcc-Ag-ZnO-Ag transistor.

mainly depend on the width of piezocharge distribution, piezoelectric semiconductor materials and electrode metal materials. The first principle simulations can provide quantitative information about the width of the piezocharge distribution, which may guide the design of piezotronic devices.

Acknowledgment

This work was supported by the "thousands talents" program for pioneer researcher and his innovation team, China, and Beijing Municipal Commission of Science and Technology (No. Z131100006013005 and Z131100006013004).

Appendix A. Supplementary Information

Supplementary data associated with this article can be found in the online version at http://dx.doi.org/10.1016/j.nanoen.2014.10.014.

Please cite this article as: W. Liu, et al., First principle simulations of piezotronic transistors, Nano Energy (2014), http://dx.doi.org/10.1016/j.nanoen.2014.10.014

References

[1] Z.L. Wang, J.H. Song, Science 312 (2006) 242.
[2] Z.L. Wang, Adv. Mater. 19 (2007) 889.
[3] Z.L. Wang, Nano Today 5 (2010) 540.
[4] Z.L. Wang, Piezotronics and Piezo-Phototronics, Springer, Berlin, Heidelberg, 2013.
[5] X.D. Wang, J. Zhou, J.H. Song, J. Liu, N.S. Xu, Z.L. Wang, Nano Lett. 6 (2006) 2768.
[6] W.H. Han, Y.S. Zhou, Y. Zhang, C.Y. Chen, L. Lin, X. Wang S.H. Wang, Z.L. Wang, ASC Nano 6 (2012) 3760.
[7] W.Z. Wu, Y.G. Wei, Z.L. Wang, Adv. Mater. 22 (2010) 4711.
[8] W.Z. Wu, Z.L. Wang, Nano Lett. 11 (2011) 2779.
[9] C.F. Pan, S.M. Niu, Y. Ding, L. Dong, R.M. Yu, Y. Liu, G. Zhu Z.L. Wang, Nano Lett. 12 (2012) 3302.
[10] Q. Yang, Y. Liu, C.F. Pan, J. Chen, X.N. Wen, Z.L. Wang, Nano Lett. 13 (2013) 607.
[11] R. Yu, C. Pan, J. Chen, G. Zhu, Z.L. Wang, Adv. Funct. Mater. 23 (2013) 5868.
[12] S. Niu, Y. Hu, X. Wen, Y. Zhou, F. Zhang, L. Lin, S. Wang Z.L. Wang, Adv. Mater. 25 (2013) 3701.
[13] C.F. Pan, R.M. Yu, S.M. Niu, G. Zhu, Z.L. Wang, ACS Nano 7 (2013) 1803.
[14] Q. Yang, W.H. Wang, S. Xu, Z.L. Wang, Nano Lett. 11 (2011) 4012.
[15] W.Z. Wu, X.N. Wen, Z.L. Wang, Science 340 (2013) 952.
[16] C.F. Pan, L. Dong, G. Zhu, S.M. Niu, R.M. Yu, Q. Yang, Y. Liu Z.L. Wang, Nat. Photo 7 (2013) 752.
[17] W.Z. Wu, C.F. Pan, Y. Zhang, X.N. Wen, Z.L. Wang, Nano Today 8 (2013) 619.
[18] Y. Gao, Z.L. Wang, Nano Lett. 7 (2007) 2499.
[19] Y. Gao, Z.L. Wang, Nano Lett. 9 (2009) 1103.
[20] Y. Zhang, Y.F. Hu, S. Xiang, Z.L. Wang, Appl. Phys. Lett. 97 (2010) 033509.
[21] Y. Zhang, Y. Liu, Z.L. Wang, Adv. Mater. 23 (2011) 3004.
[22] X. Luo, B. Wang, Y. Zheng, ACS Nano 5 (2011) 1649.
[23] G.H. Zhang, X. Luo, Y. Zheng, B. Wang, Phys. Chem. Chem. Phys. 14 (2012) 7051.
[24] S. Kasamatsu, S. Watanabe, S. Han, Phys. Rev. B. 84 (2011) 085120.
[25] Y.F. Dong, L.J. Brillson, J. Electron. Mater. 37 (2008) 743.
[26] B. Meyer, D. Marx, Phys. Rev. B. 69 (2004) 235420.
[27] A. Zaoui, Phys. Rev. B. 69 (2004) 115403.
[28] T. Kamiya, K. Tajima, K. Nomura, H. Yanagi, H. Hosono, Phys. Status Solidi A. 205 (2008) 1929.
[29] J.P. Perdew, K. Burke, M. Ernzerhof, Phys. Rev. Lett. 77 (1996) 3865.
[30] G. Kresse, J. Hafner, Phys. Rev. B. 48 (1993) 13115.
[31] G. Kresse, J. Furthmuller, Phys. Rev. B. 54 (1996) 11169.
[32] P.E. Blöchl, Phys. Rev. B. 50 (1994) 17953.
[33] G. Kresse, D. Joubert, Phys. Rev. B. 59 (1999) 1758.
[34] N. Troullier, J.L. Martins, Phys. Rev. B. 43 (1991) 1993.
[35] N.A. Pertsev, A.G. Zembilgotov, A.K. Tagantsev, Phys. Rev. Lett. 80 (1998) 1988.
[36] L. Colombo, R. Resta, S. Baroni, Phys. Rev. B. 44 (1991) 5572.
[37] J. Junquera, M.H. Cohen, K.M. Rabe, J. Phys-Condens. Mat 19 (2007) 213203.
[38] C.G. Van de Walle, R.M. Martin, Phys. Rev. B. 34 (1986) 5621.
[39] M. Peressi, N. Binggeli, A. Baldereschi, J. Phys. D. 31 (1998) 1273.
[40] S.H. Wei, A. Zunger, Phys. Rev. Lett. 59 (1987) 144.
[41] J. Zhou, Y.D. Gu, P. Fei, W.J. Mai, Y.F. Gao, R.S. Yang, G. Bao, Z.L. Wang, Nano Lett. 8 (2008) 3035.

Dr. **Wei Liu** received his Ph. D degree from The University of Tokyo in 2012. After graduation, he joined the Beijing Institute of Nanoenergy and Nanosystems as an assistant researcher. His research interests include first principle simulation on piezotronic devices and ac output of nanogenerators.

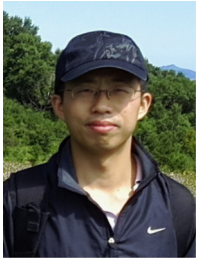

Dr. **Aihua Zhang** received his Ph. D degree From Tsinghua University in 2006. After graduation, he worked as postdoctoral researchers in Fritz-Haber-Institut der Max-Planck-Gesellschaft in Germany and National University of Singapore. He joined the Beijing Institute of Nanoenergy and Nanosystems as an assistant researcher in 2013. His research interests are size-effect in piezotronics and first principle simulation of piezo-magnetotronics.

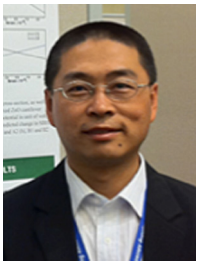

Dr. **Yan Zhang** received his B. S. degree (1995) and Ph.D degree in Theoretical Physics (2004) from Lanzhou University. Then, he worked as a lecturer, associate Professor (2007), and Professor (2013) of Institute of Theoretical Physics in Lanzhou University. In 2009 he worked as research scientist in the group of Professor Zhong Lin Wang at Georgia Institute of Technology. His main research interest and activities are: self-powered nano/micro system, theoretical calculation of piezotronic, dynamics of time-delay systems and complex networks.

Zhong Lin (ZL) Wang received his Ph.D. from Arizona State University in physics. He now is the Hightower Chair in Materials Science and Engineering, Regents' Professor, Engineering Distinguished Professor and Director, Center for Nanostructure Characterization, at Georgia Tech. Dr. Wang has made original and innovative contributions to the synthesis, discovery, characterization and understanding of fundamental physical properties of oxide nanobelts and nanowires, as well as applications of nanowires in energy sciences, electronics, optoelectronics and biological science. His discovery and breakthroughs in developing nanogenerators established the principle and technological roadmap for harvesting mechanical energy from the environment and biological systems for powering a personal electronics. His research on self-powered nanosystems has inspired the worldwide effort in academia and industry for studying energy for micro-nano-systems, which is now a distinct disciplinary in energy research and future sensor networks. He coined and pioneered the field of piezotronics and piezo-phototronics by introducing piezoelectric potential gated charge transport process in fabricating new electronic and optoelectronic devices. Details can be found at: http://www.nanoscience.gatech.edu.

Please cite this article as: W. Liu, et al., First principle simulations of piezotronic transistors, Nano Energy (2014), http://dx.doi.org/10.1016/j.nanoen.2014.10.014